Acta Scientiarum
http://periodicos.uem.br/ojs
ISSN on-line: 1807-8664
Doi: 10.4025/actascitechnol.v46i1.66904

Lipid microcapsule synthesis from *Melaleuca alternifolia* (tea tree) hydrolate

Creir da Silva[1], Cristiane Mengue Feniman Moritz[2], Paulo Rodrigo Stival Bittencourt[3], Angela Maria Picolloto[2], Leandro Ferreira Pinto[4], Paulo Cardozo Carvalho de Araújo[5], Otávio Akira Sakai[1] and Osvaldo Valarini Junior[6*]

[1]Instituto Federal do Paraná, Umuarama, Paraná, Brazil. [2]Universidade Estadual de Maringá, Maringá, Paraná, Brazil. [3]Universidade Tecnológica Federal do Paraná, Medianeira, Paraná, Brazil. [4]Universidade Estadual Paulista, Faculdade de Engenharia e Ciências, Rosana, São Paulo, Brazil. [5]Departamento de Engenharia Química, Universidade de São Paulo, São Paulo, São Paulo, Brazil. [6]Departamento Acadêmico de Engenharia Química e de Alimentos, Universidade Tecnológica Federal do Paraná, Via Rosalina Maria dos Santos, 1233, 87301-899, Campo Mourão, Paraná, Brazil. *Author for correspondence. E-mail: osvaldovalarini@utfpr.edu.br

ABSTRACT. This study aimed to use *Melaleuca alternifolia* hydrolate to produce and optimize microparticles via three microemulsion processes: simple hot; ultrasonic; and double. Surfactants, including stearic acid, lecithin and Tween 80 were utilized in these processes. Experimental diameters were optimized using a 2^2 factorial planning of response surfaces. The smallest experimental mean diameters were obtained by R4 simple hot microemulsion with lecithin, R7 simple hot microemulsion with Tween 80, R4 ultrasonic microemulsion with lecithin; R4 ultrasonic microemulsion with Tween 80; and R5 double microemulsion. The latter obtained the smallest mean particle diameter of all experiments (0.65 ± 0.10 µm). All particles formed with *Melaleuca alternifolia* hydrolate obtained an isoelectric point equal to zero at pH 7. Fourier-transform infrared spectroscopy was used to characterize the best conditions of each technique. In conclusion, our findings suggest that as the system receives more energy, the mean particle diameter tends to decrease.

Keywords: *Melaleuca alternifolia* by-product; microemulsion; ultrasonication; double emulsion; optimization.

Received on January 30, 2023.
Accepted on January 9, 2024.

Introduction

The search for alternatives to replace synthetic or polluting products has significantly grown, especially for herbal products. Many plants may compose secondary metabolites to inhibit pathogenic microorganisms, agricultural plagues and predators. *Melaleuca* is a shrubby from Myrtaceae family, which contains more than 230 catalogued species. *Melaleuca alternifolia*, which is popularly known as tea tree, originates from swampy regions in northeastern and southeastern Australia, and mature specimens of this species can stand above 6 m (Patil, Chandra, Jayanthi, Shirahatti, & Ramu, 2021).

Westerners only discovered this specific Myrtaceae species in 1770, after James Cook's expedition to Botany Bay, in New South Wales, during which he observed native people using plant leaves in medicinal rituals. However, the first scientific publication proving the antimicrobial capacity of its essential oil (tea tree oil - TTO) emerged in 1923. Since then, numerous other scientific studies have assessed the different medicinal uses of TTO (Naccari, Cicero, Orlandella, Naccari, & Palma, 2023; Upadhyay, Malik, & Upadhyay, 2023).

TTO is the main marketed *Melaleuca alternifolia* product, obtained by hydro- and steam distillation, and produced on an industrial scale in Australia. Its chemical composition contains terpene hydrocarbons, monoterpenes, sesquiterpenes and associated alcohols with antimicrobial, anti-inflammatory, and antioxidant functions — although it may be altered due to oxygen, light, heat, moisture exposure and storage time, among other factors (Voelker, Mauleon, & Shepherd, 2023; Zhang, Guo, Guo, Jiang, & Ji, 2018).

The hydrolate is generated in large quantities (99%) during the hydro/steam distillation process to obtain TTO. It is a little explored by-product, which has a small amount of essential oil (around 1%) dissolved, in which oxygenated compounds with organoleptic properties are found (Aćimović et al., 2020). These factors directly influence the quality and shelf life of essential oils, and thus, this research has sought new methods of stocking these products. Encapsulation is one of several alternatives to preserve the useful life of chemical compounds. It can prolong storage and control the release of encapsulated compounds during use (Houghton, 2004; Xu et al., 2022).

Lipid capsules occur by forming a film around its active ingredient. Its production consists of mixing lipids, water, and surfactants, it interacts well with essential oils and is more affordable than other storage techniques. Lipid capsules have sizes ranging from 10 to 1000 nm, consist of solid lipids, show physical stability, it can incorporate thermolabile drugs, are solid in colloidal dispersions, have large surfaces, and can interact with other drugs (Mohite, Singh, Pawar, Sangale, & Prajapati, 2023). As advantage, they can be stored as solids and used with natural solvents. Their disadvantages include drug requirement for polymer movement, the unpredictable gelling process, and their suboptimal suitability for hydrophilic drugs (Musakhanian, Rodier, & Dave, 2022).

Microemulsions are techniques that can dissolve drugs. Double microemulsions contribute to the storage of hydrophilic drugs and provide high encapsulation efficiency (Hatefi & Farhadian, 2020). Hot microemulsions occur at temperatures above the melting temperature of lipid, and are simple and inexpensive. However, they heterogeneously distribute particle size. Microemulsion followed by ultrasonication reduces size range and sheer size, but contaminates samples with metals and causes the growth of physically unstable particles (Ma, Varanda, Perussi, & Carrilho, 2021).

The production of nanostructures with better physicochemical and biological properties finds extensive applications in pharmaceutical, cosmetic, and food industries. The industry has taken great interest in nanoemulsions and nanostructures with lipid carriers due to their bio-availability, solubility improvement, and bioactive stabilization (Reis et al., 2020).

This study aimed to analyze the average particle diameter and surface load of lipid microparticle capsules produced from three different techniques using *Melaleuca* hydrolate. It holds the potential to make significant contributions to the field of nanotechnology and enhance our fundamental understanding of the chemical compounds present in hydrolates for the development of microparticle capsules. These findings may further contribute to the innovation of new cosmetics.

Material and methods

Materials

Baerlocher (Brazil) stearic acid, Adicel (Brazil) lecithin, and Sigma-Aldrich (USA) Tween 80 reagents were used. The hydrolate was obtained from TTO extraction residues via hydrodistillation using a Clevenger-type device, with 40 g of leaves and 250 mL of distilled water for 1.5 hours. A magnetic mixer and thermostatic bath from Global Equipamento Techology (Brazil), a Ultrasonifier UCD-90 Model from Biobase Biodustry (China), and (to form particles) the TE-102 Turratec from Tecnal (Brazil) were used.

Preparation of solid lipid nanoparticles

Microparticles were prepared via microemulsion, microemulsion followed by ultrasonication, and double microemulsions.

The microparticles produced by hot microemulsion were adapted for this study (de Sousa & Pessine, 2014; Ife, Harding, Shah, Palombo, & Eldridge, 2018). From the heavy mass of stearic acid and the surfactants lecithin or Tween 80, stearic acid and a surfactant were added to a beaker. The microparticles formed by microemulsion followed by ultrasonication were adapted to this study (Behbahani, Ghaedi, Abbaspour, & Rostamizadeh, 2017). Stearic acid and surfactants were weighed according to microemulsion (Table 1).

Table 1. Experimental design for microlipid synthesis by microemulsion and microemulsion followed by ultrasonication for (x_1) stearic acid (x_2) $Ratio_{Stearic\ Acid/Surfactant}$.

Run	Stearic Acid (%w/0.1 v) (x_1)	$Ratio_{Stearic\ Acid/Surfactant}$ (x_2)
R1	0.30 (-1)	1.00 (-1)
R2	0.30 (-1)	3.00 (1)
R3	0.90 (1)	1.00 (-1)
R4	0.90 (1)	3.00 (1)
R5	0.18(-1.41)	2.00 (0)
R6	1.02 (1.41)	2.00 (0)
R7	0.60 (0)	0.59(-1.41)
R8	0.60 (0)	3.41 (1.41)
R9	0.60 (0)	2.00 (0)
R10	0.60 (0)	2.00 (0)

Then, 10 mL of *Melaleuca alternifolia* hydrolate were added to another beaker. Samples were kept in thermostatic baths at 353 K (Shah, Eldridge, Palombo, & Harding, 2017) due to the melting point of steric acid (Coşanay, Selimefendigil, Öztop, & Sarı, 2022). Then, samples were mixed and stirred in the TE-102 Turratec for 5 min. at 3200 rpm (Figure 1a$_1$). A 1:10 proportion of hot:cold systems were used (de Sousa & Pessine, 2014) Within the TE-102 Turratec, *Melaleuca alternifolia* hydrolate was dripped at 700 rpm at 0-3 K in the formed capsules and *Melaleuca alternifolia* hydrolate/stearic acid/surfactants were stirred for 15 min. (de Sousa & Pessine, 2014) (Figure 1a$_1$). Reagents were mixed and stirred for 05 min. at 1500 rpm and at 353 K constant temperature in a magnetic mixer (Figure 1a$_2$). In a ultrasonifier (model UCD-90, 1000 W with 1/2''tip), reagents were mixed and stirred for 60 seconds at 2% amplitude under a sonified 10-s pulse regime and 5-s pause. The sample was cooled in a magnetic mixer at the same proportion, speed, and time as the microemulsion.

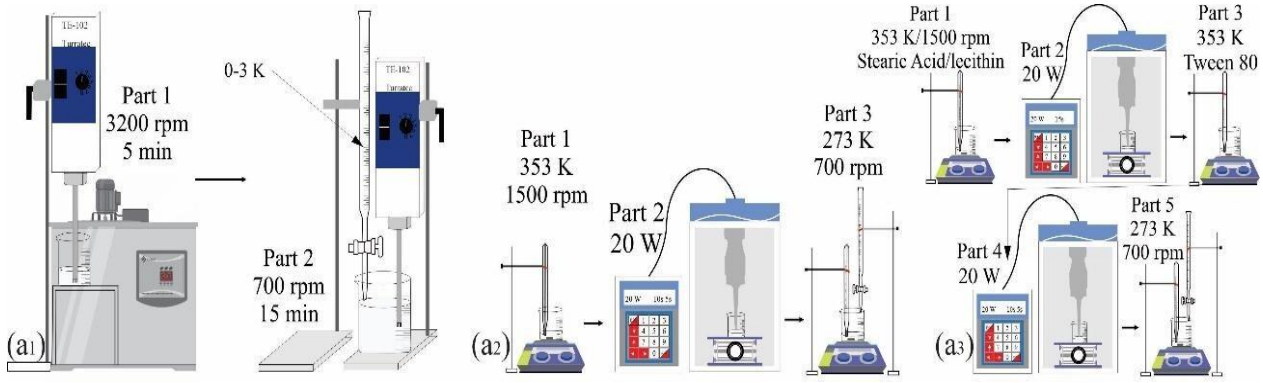

Figure 1. Schematization of the techniques of microemulsion (a$_1$), microemulsion followed by ultrasonication (a$_2$), and double emulsion ultrasonication (a$_3$).

Double emulsion (Figure 1a$_3$) was based on the technique developed by (Becker Peres, Becker Peres, Araújo, & Sayer, 2016; Hatefi & Farhadian, 2020), in which the stearic acid and lecithin (internal phase) were weighed (Table 2).

Table 2. Experimental design for synthesis of microlipid by microemulsion by double emulsion for (x_1) stearic acid (x_2) Ratio$_{\text{Stearic Acid/Surfactant}}$.

Run	Stearic Acid (g) x_1	Ratio$_{\text{External Surfactant/ internal}}$ by Stearic Acid x_2
R1	0.30 (-1)	5.00 (-1)
R2	0.30 (-1)	15.00 (1)
R3	0.90 (1)	5.00 (-1)
R4	0.90 (1)	15.00 (1)
R5	0.18 (-1.41)	10.00 (0)
R6	1.02 (1.41)	10.00 (0)
R7	0.60 (0)	2.93 (-1.41)
R8	0.60 (0)	17.07 (1.41)
R9	0.60 (0)	10.00 (0)
R10	0.60 (0)	10.00 (0)

The mixtures of the internal phase were placed in a beaker and taken to a magnetic mixer at a 353 K temperature, with the same procedure being carried out for 10 mL of *Melaleuca alternifolia* hydrolate. Then, they were mixed at 353 K, and placed in a ultrasonifier (UCD-90 model, 1000 W with a 1/2''tip) for 15 seconds of continuous sonication at 2% amplitude. Then, a mixture of 6 mL of the *Melaleuca alternifolia* hydrolate and Tween 80 (External phase) was added. The sample was homogenized and taken to a ultrasonifier for 60 seconds (2% amplitude in a 10-s sonified and 5-s pause regime). The sample was cooled at a 1:10/hot:cold ratio. Finally, *Melaleuca alternifolia* hydrolate was dripped in the formed capsules for 15 min. in a magnetic mixer at 0-3 K and at 700 rpm (de Sousa & Pessine, 2014).

Characterization

A 2^2 duplicated factorial design for independent central points was used in this study. In total, two variables and levels were investigated. Overall, 10 experiments were required for each technique. A second-

order model curvature is usually required to adjust responses, constituting the most suitable adjustment in most cases (Iwundu & Oko, 2021; Montgomery, 2012).

$$y = \beta_0 + \sum_{i=1}^{k} \beta_i x_i + \sum_{i=1}^{k} \beta_i x_i^2 + \sum \sum_{i<j} \beta_{ij} x_i x_j + \in \quad (1)$$

Factors were defined as lower (-1), upper (1), central (0), and extreme (-1.41, 1.41) for our curvature adjustment. In this study, stearic acid (x_1) and its ratio per surfactant (x_2) were analyzed. Stearic acid ranged from 0.3 to 0.9, and surfactants from 1 to 3 for microemulsion and ultrasonic microemulsion (Montgomery, 2012). The same stearic acid proportion was used for double microemulsions, but surfactants were used from a 1/5 internal to 1/10 external ratio, based on studies on the assessed techniques. Our experimental design was used to optimize d_{exp} response. Polynomial equations are obtained by factor dependence and independence. A 5% significance was defined for the difference between the mean values of the tested parameters (Valarini Junior, Cardoso, Machado Giufrida, de Souza, & Cardozo-Filho, 2019).

The d_{exp} was measured by the Litesizer TM 500 Anton Paar (Austria). Measurements were performed by diluting samples in deionized water in a 1:10 ratio (Yamamoto et al., 2023). Parameters determined by our measurements were automatically chosen by Litesizer TM 500. Zeta potential was determined in an electrolyte cell, which was measured at pH = 7. Results were obtained by particle movement due to the electric field applied at cell extremities. All variables were measured in triplicates (Valarini Junior et al., 2019; Cardoso, Souza, Machado Giufrida, Cardozo-Filho, 2021).

Microcapsules were also analyzed by a spectrophotometer (Cary 630 model, Agilent Technologies) in 128 scans with a 2 cm^{-1} spectral resolution. Typical bands were recorded from 3500 to 400 cm^{-1}.

Results and discussion

Finding the physicochemical parameters that influence capsules and affect the pharmaceutical properties of host molecules is of great importance for new formulations. To attain the most favorable d_{exp}, we employed a 2^2 factorial planning, as presented in Tables 3, 4 and 5.

Table 3. Experimental diameters for microlipid synthesis by microemulsion for (x_1) stearic acid (x_2) $Ratio_{Stearic\ Acid/Surfactant}$.

Run	Lecithin			Tween 80		
	d_{exp} (μm)	PDI	Zeta potential (mV) ±0.02	d_{exp} (μm)	PDI	Zeta potential (mV) ±0.02
R1	1.02±0.12	0.18	-0.03	0.74±0.09	0.26	-0.01
R2	1.97±0.17	0.24	-0.02	1.83±0.16	0.22	-0.01
R3	1.15±0.23	0.25	-0.02	1.13±0.12	0.26	-0.01
R4	0.80±0.09	0.27	-0.02	3.00±0.19	0.25	-0.01
R5	2.26±0.14	0.23	-0.02	1.03±0.12	0.26	-0.02
R6	0.80±0.11	0.25	-0.03	0.66±0.10	0.12	-0.01
R7	1.80±0.16	0.27	-0.03	0.79±0.08	0.13	-0.02
R8	1.70±0.21	0.17	-0.02	3.06±0.22	0.40	-0.01
R9	1.17±0.16	0.25	-0.02	1.52±0.17	0.21	-0.01
R10	1.61±0.14	0.22	-0.02	1.40±0.13	0.17	0.01

Table 4. Experimental diameters for microlipid synthesis by microemulsion ultrasonication for (x_1) stearic acid (x_2) $Ratio_{Stearic\ Acid/Surfactant}$.

Run	Lecithin			Tween 80		
	d_{exp} (μm)	PDI	Zeta potential (mV) ±0.02	d_{exp} (μm)	PDI	Zeta potential (mV) ±0.02
R1	1.80±0.21	0.27	-0.02	1.18±0.23	0.24	-0.02
R2	1.22±0.18	0.19	-0.02	0.80±0.14	0.24	-0.02
R3	3.44±0.23	0.59	-0.03	1.43±0.19	0.28	-0.02
R4	0.49±0.14	0.30	-0.03	1.28±0.13	0.38	-0.02
R5	0.73±0.23	0.41	-0.02	1.20±0.27	0.38	-0.02
R6	2.59±0.18	0.36	-0.03	0.90±0.17	0.18	-0.02
R7	2.90±0.26	0.38	-0.03	1.69±0.18	0.35	-0.02
R8	1.30±0.26	0.34	-0.02	0.88±0.14	0.04	-0.03
R9	1.02±0.33	0.35	-0.02	1.70±0.23	0.27	-0.02
R10	0.87±0.21	0.29	-0.02	1.76±0.28	0.18	-0.02

Table 5. Experimental diameters for microlipid synthesis by microemulsion by double emulsion for (x_1) stearic acid (x_2) $Ratio_{Stearic\ Acid/Surfactant}$.

Run	d_{exp} (µm)	PDI	Zeta potential (mV) ±0.02	d_{exp} (µm)
R1	1.52 ± 0.12	0.19	- 0.02	1.18±0.23
R2	1.01 ± 0.13	0.22	- 0.03	0.80±0.14
R3	2.54 ± 0.25	0.21	-0.02	1.43±0.19
R4	1.85 ± 0.18	0.15	- 0.03	1.28±0.13
R5	0.65 ± 0.10	0.21	- 0.03	1.20±0.27
R6	3.54 ± 0.26	0.24	- 0.03	0.90±0.17
R7	1.50 ± 0.21	0.20	-0.02	1.69±0.18
R8	0.75 ± 0.09	0.19	- 0.03	0.88±0.14
R9	0.87 ± 0.16	0.22	- 0.03	1.70±0.23
R10	0.90 ± 0.14	0.25	-0.03	1.76±0.28

The surface response methodology was applied to transform variables into factors and optimize our experiments (e.g., response variables) (Montgomery, 2012; Valarini Junior et al., 2019). Stationary point location is of great importance for the best x_1 and x_2 conditions and their interactions to optimize our surface response methodology. It illustratively optimizes responses via maximum, minimum or cell points. Moreover, contour charts play an important role in response surface studies (Montgomery, 2012).

The planning results show the importance of optimizing experiments and reaffirm their statistical importance. The surface response methodology was applied to determine the factor levels interfering with d_{exp}. Tables 6, 7 and 8 show the p-value coefficients, which have a 0.05 significance effect on our predictive model. Turning variables into factors is important in surface response methodology (Pinto, Barros, Reis, & Fonseca, 2019; Valarini Junior et al., 2019).

Table 6. Significance test, standard-error and the respective confidence interval of the microemulsion and d_{exp} parameter estimates (µm). Combined regression variables were analyzed for Stearic Acid-x_1 and $Ratio_{stearic\ acid/surfactant}$-$x_2$, respectively.

Variable	Lecithin				Tween 80			
	d_{exp} (µm)	p-value	Standard-error	Confidence interval	d_{exp} (µm)	p-value	Standard-error	Confidence interval
A	1.39	0.007	0.279	0.614-2.166	1.46	0.010	0.319	0.573-2.347
x_1	-0.77	0.049	0.139	-0.776–(-0.001)	0.26	0.462	0.160	-0.314-0.573
x_2	0.11	0.703	0.139	-0.330-0.445	-1.61	0.007	0.160	0.363-1.250
$x_1\ x_2$	-0.65	0.175	0.197	-0.874-0.223	-0.39	0.436	0.226	-0.432-0.822
x_1^2	0.06	0.874	0.185	-0.554-0.488	-0.44	0.351	0.211	-0.809-0.364
x_2^2	0.16	0.692	0.184	-0.434-0.591	-0.53	0.274	0.211	-0.319-0.854

Table 7. Significance test, standard-error and the respective confidence interval of the microemulsion ultrasonication and d_{exp} parameter estimates (µm). Combined regression variables were analyzed for Stearic Acid-x_1 and $Ratio_{stearic\ acid/surfactant}$-$x_2$, respectively.

Variable	Lecithin				Tween 80			
	d_{exp} (µm)	p-value	Standard-error	Confidence interval	d_{exp} (µm)	p-value	Standard-error	Confidence interval
A	0.94	0.027	0.279	0.170-1.719	1.73	0.000	0.164	1.274-2.185
x_1	0.88	0.034	0.139	0.055-0.829	0.08	0.666	0.082	-0.189-0.266
x_2	-1.45	0.006	0.139	-1.111-(-0.336)	-0.42	0.063	0.082	-0.437-0.018
$x_1\ x_2$	-1.18	0.039	0.184	-1.140-(-0.448)	-0.11	0.646	0.11	-0.265-0.380
x_1^2	0.64	0.156	0.184	-0.190-0.834	-0.68	0.035	0.109	-0.640-(-0.037)
x_2^2	1.08	0.042	0.197	0.029-1.054	-0.44	0.111	0.109	-0.523-0.080

Table 8. Significance test, standard-error and the respective confidence interval of the double emulsion and d_{exp} parameter estimates (µm). Combined regression variables were analyzed for Stearic Acid-x_1 and $Ratio_{stearic\ acid/surfactant}$-$x_2$, respectively.

Variable	d_{exp} (µm)	p-value	Standard-error	Confidence interval
A	0.88	0.036	0.288	0.092-1.677
x_1	1.48	0.006	0.142	0.347-1,134
x_2	-0.56	0.118	0.142	-0,678-0.113
$x_1\ x_2$	-0.09	0.834	0.207	-0.603-0.513
x_1^2	1.27	0.028	0.187	0.110-1.159
x_2^2	0.30	0.471	0.187	-0.374-0.674

The experimental responses encoded by factors x_1 and x_2 can also be represented by general mathematical solutions which locate the stationary points, with p-value < 0.05, such as equations (2-6).

$$d_{exp,\ Lecithin,Microemulsion}\ (\mu m) = 1.39 - 0.77x_1 \quad (2)$$

$$d_{exp,\ Tween,\ Microemulsion}\ (\mu m) = 1.46 + -1.61x_2 \quad (3)$$

$$d_{exp,\ Lecithin,\ Ultrasonication}\ (\mu m) = 0.94 + 0.88x_1 - 1.45x_2 - 1.18x_1x_2 + 1.08x_2^2 \quad (4)$$

$$d_{exp,\ Tween,\ Ultrasonication}\ (\mu m) = 1.73 \quad -0.68x_1^2 \quad (5)$$

$$d_{exp,\ Double\ Emulsion}\ (\mu m) = 0.88 + 1.48x_1 + 1.27x_1^2 \quad (6)$$

The equations (2-6) show three techniques with two surfactants each, offering a singular analysis of each equation associated with its respective graph. Equation (2) shows that the d_{exp} midpoint is at 1.39 µm. The only factor that interferes in this equation is first order stearic acid. In the equation (3), the surfactant was changed to analyze the particle size (response variable) using Tween 80, and the significant factor is $Ratio_{External\ Surfactant\ internal}$ by Stearic Acid of first order. Equation (4) is the one with the greatest significance among the factors. This may be associated with a better interaction of the reagents with the ultrasonication technique, which provides greater energy to the system. Equation (5) also used the ultrasonication technique, in which the factors did not reach the same significance as the factors in equation (4). The technique used with the Tween 80 reagent did not obtain the same interaction as lecithin. This may be associated with the chemical properties of the compounds. Equation (6) shows that the first and second order factors of stearic acid are significant.

The stearic acid estimated p-value shows that only its midpoint and linear x-factor is significant for planning (Tables 5-8). Thus, only the amount of stearic acid interferes with microparticle capsules. Table 3 shows that the increase in the amount of stearic acid decreases $d_{exp,}$ and that the stearic acid ratio per surfactant failed to significantly interfere with d_{exp}. In runs R4 and R6, the changes in the surfactant quantity resulted in the observation of 0.80 µm d_{exp}.

Figure 2a shows that the closer to the stationary dark green region, the smaller the d_{exp}. This means that the best region to obtain small particles lies between 1.0 and 1.1 of stearic acid at 3.0 to 4.0 of its ratio to surfactant. Table 3 shows that R4 and R6 obtained a 0.80 µm d_{exp}.

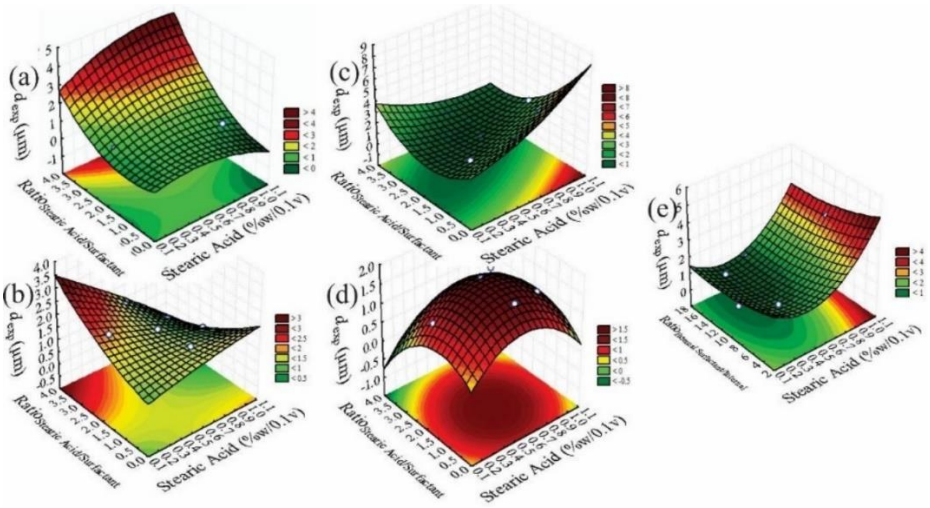

Figure 2. RSM plot of the microemulsions. (a_1) Microemulsion with lecithin. (b_1) RSM Microemulsion with Tween 80. (c_1) Ultrasonication with lecithin. (d_1) Ultrasonication. (e_1) Double emulsion ultrasonication.

This equation has a higher midpoint than equation (2), increasing 0.07 µm than the same technique with another surfactant. However, the d_{exp} of some runs were smaller than the diameters of lecithin microemulsions. R1, R6, and R7 had smaller d_{exps} than any lecithin experiment. R7 showed the lowest d_{exp}. Figure 2b confirms these experiments by intersecting the ordinate between 2.5 and 4.0 and x values between 1.05 and 1.1, giving us the R1, R6, and R7 d_{exp}. Midpoint and linear x_2 were the significant factors (Table 5). This shows that the ratio between stearic acid and surfactant interferes with d_{exp}. The 0.07 µm difference may relate to surfactant modification.

Size difference may be due to the hydrophilic balance of lecithin and Tween 80. Lecithin has a hydrophilic balance = 8 (Hatefi & Farhadian, 2020). It is hydrophilic due to the phosphate head of its molecule, and hydrophobic due to its fatty acids, strongly influencing its oil partition coefficient in water (McClements, 2020). Fatty acid micelles form a nucleus which protects the host molecule (Bot, Cossuta, & O'Mahony, 2021). Particle formation efficiency directly relates to the technique. High-energy methods facilitate droplet fragmentation within the high-energy homogenizer, whose particle size ranges from 0.2 to 0.8 µm (Komaiko, Sastrosubroto, & McClements, 2015). Tween 80 is a non-ionic surfactant due to its hydrophilic balance = 15 (Lian, Peng, Shi, & Wang, 2019). Hydrophilic balances larger than 13 result in a clear solution (Gadhave, 2014). Tween 80 has good lipid nanoparticle functionalization and stabilization. Thus, lipid nanostructures widely use it (de Souza, Saez, Campos, & Mansur, 2019), which may further decrease particle size and d_{exp} than lecithin.

The best conditions for ultrasonic microemulsion consisted of R4=0.49±0.14 µm with lecithin and R2 = 0.80±0.14 µm with Tween 80 (Table 2). In this technique, lecithin obtained a smaller d_{exp} than Tween 80. Size difference may relate to several factors such as ultrasonication length and intensity, lipids, liquids, surfactants, and concentrations (de Souza et al., 2019). Several authors also found a decrease in d_{exp} as lecithin concentrations increased by several homogenization methods (Komaiko et al., 2015). This is evident in equations (4-5).

Almost all of equation (4) is significant (Table 4), except for x_1^2. Thus, experiment conditions, such as ultrasonication and reagent mass factorially interacted. Linear $x_1.x_2$, quadratic x_1, and $x_1.x_2$ interaction justify reagent interaction, which even explains the harmony between them. It may only occur in ultrasonic microemulsions. Furthermore, the homogenization followed by ultrasonication is better to obtain homogeneous distributed particles (de Souza et al., 2019). Figure 2c shows that the stationary point occurs at the intersection 0.4-0.7 on the abscissa, and at 2.2-3.0 on the ordinate. Values of this replaced range in equation (4) will result in a d_{exp} very close to condition R4. Equation (4) obtained the best adjustment (R-adj = 0.93).

Ultrasonication with Tween 80 generated larger sizes than with lecithin. This may be related to the interaction between technique and surfactant. Some authors report that the high concentration of surfactants in lipid nanoparticles facilitates partitioning during emulsification (de Souza et al., 2019). The significant parameters in this condition were the midpoint and x_1 squared. However, in this type of system, it is not possible to infer true surfaces or stationary points, since the optimal points are outside the model´s adjustment (Montgomery, 2012).

Equation (6) shows that the midpoint of its d_{exp} is 0.88 µm. The estimated p-value in this equation shows that only its midpoint and its linear and quadratic x_1 factor are significant for planning (Table 7), with a 0.92 correlation coefficient. Thus, only stearic acid influences d_{exp}. Table 5 shows that increasing stearic acid at extreme points interfered with d_{exp} and that surfactant ratio to stearic acid failed to significantly affect d_{exp}. The best condition obtained in this study was R5.

Figure 2e shows that the best conditions on the x and y axes are intersected in the dark green region (smaller d_{exp}). This means that the best region for small particles lies between 0.35 and 0.45 of stearic acid and a ratio of 12 to 16 (y-axis) of surfactant between its external and internal phases. Thus, by replacing these values in equation (6), values very close to R5 are obtained. The best d_{exp} was at 277 nm at a 1/10 lecithin/Tween 80 ratio for 0.3 g (Becker Peres et al., 2016). The best condition was achieved when the lowest mass was obtained.

Thus, the 1/10 lecithin/Tween 80 ratio was the best condition. The greater d_{exp} than the obtained in our previous study may be related to the amount of water added in the first emulsion and its substitution for *Melaleuca alternifolia* hydrolate. Due to our first hypothesis, we used 10 mL of hydrolate instead of 200 µL. In our second hypothesis, the hydrolate may have altered capsule configuration by increasing its size, which is proved by the Zeta potential (Table 5-8). All runs had a Zeta equal to zero. Becker's best condition showed a– 52.7 mV Zeta potential. This induces the claim that the hydrolate altered the surface load of the microparticles.

Stearic acid, lecithin, and Tween 80 have an anionic character around -15 to -35 mV (Valarini Junior et al., 2019). When *Melaleuca* oil was used, the resulting Zeta potential approached– 8 mV (Comin et al., 2016). Consequently, its by-product, used in large quantities, induced an isoelectric point in the lipid nanoparticle at pH 7. Polydispersity values ranged from 0.12 to 0.40. As the values approach 0, the particles become more homogeneous (Suhaimi, Hisam, & Rosli, 2015).

Based on these techniques, the best condition for *Melaleuca alternifolia* hydrolate capsules was achieved with run R5 double emulsion (Figure 3).

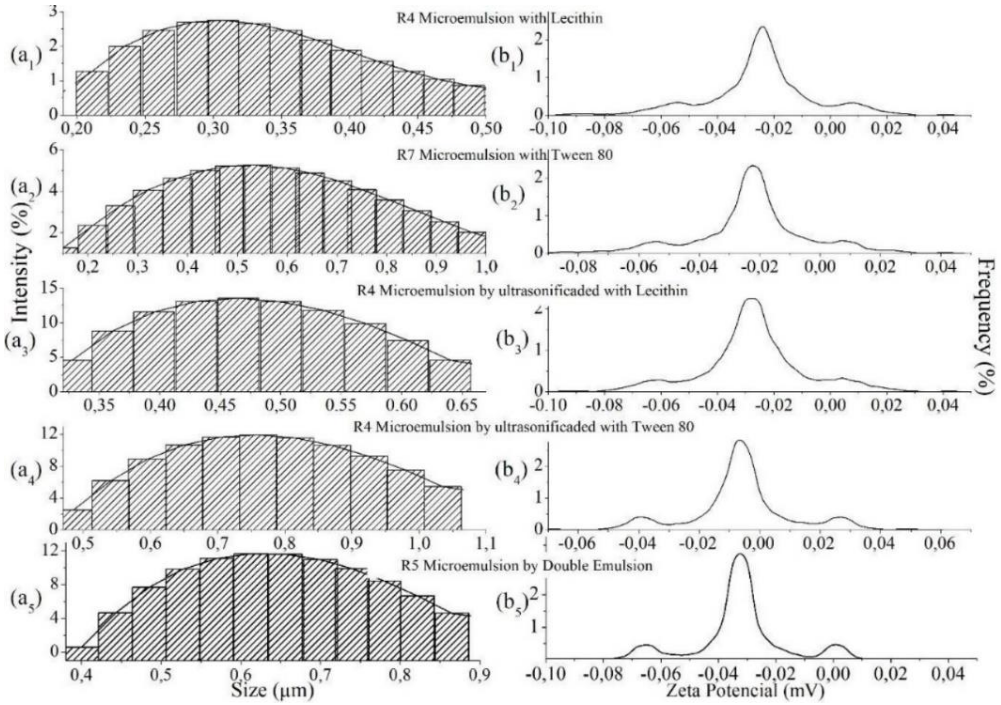

Figure 3. Experimental diameter average of microparticle and Zeta potential.

Melaleuca alternifolia hydrolate contributed to the neutrality of lipid particle charges, since all runs had the same Zeta and the reagents used have an anionic load on its surface.

Figure 4 shows the Fourier-transform infrared/attenuated total reflectance spectra of *Melaleuca* hydrolate microparticle samples via several techniques.

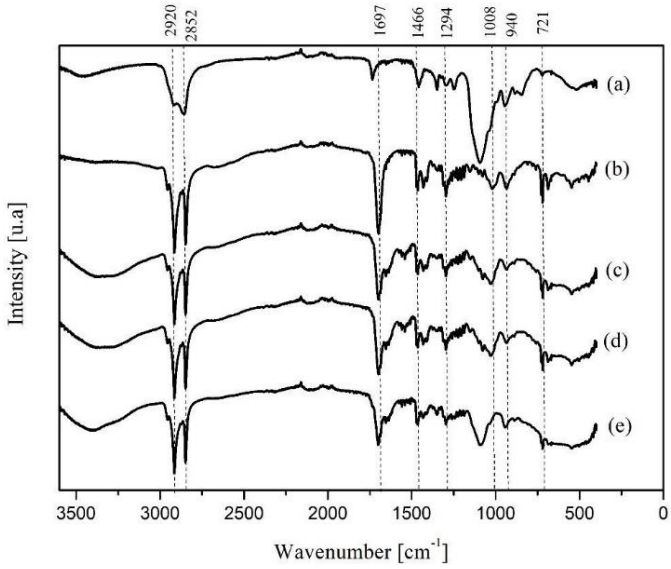

Figure 4. FT-IR of the microparticle (a) Microemulsion Double Emulsion. (b) Microemulsion with Tween 80. (c) Microemulsion with lecithin. (d) Microemulsion by ultra-sonication lecithin. (e) Microemulsion by ultra-sonication Tween 80.

The peaks of infrared light absorption and wavelengths showed small displacements during the tested particle formation techniques. *Melaleuca alternifolia* oil show 3300 cm^{-1} hydroxyl, imine, and amino bands; 1537 cm^{-1} in the C-N triazine ring stretch; and 1450 cm^{-1} and 1369 cm^{-1} C-H bending vibration in CH_2. Tween 80 bands show -CH_3 asymmetric vibrations at 1466 cm^{-1}. Stearic acid has C=O bonds at 1697 cm^{-1} (attributed to vibrational elongation, a remarkable characteristic of fatty acids), 1466 cm^{-1} CH_2 bonds, 940 cm^{-1}stearic acid spectrum peaks (O-C=O), and 1080 cm^{-1} skeletal vibration (Kumar & Randhawa, 2015). The strong bands around 2850 and 2920 cm^{-1} were assigned Alquil C-H stretch vibration (Sánchez-Navarro, Cuesta-Garrote, Arán-Áis, & Orgilés-Barceló, 2011).

Conclusion

In conclusion, particles of micrometric scale of stearic acid with the surfactants lecithin, Tween 80, or both, using *Melaleuca alternifolia* hydrolate were successfully produced by simple hot microemulsion followed by either ultrasonication or double emulsion. The three particle formation techniques changed conformational structures and surface charges. Experiment conditions enabled us to evaluate the best condition for the smallest mean particle diameter and surface isoelectric point. The R5 (which used double emulsion) showed a d_{exp} = 0.65±0.10 µm, being the condition with the smallest average particle diameter. *Melaleuca alternifolia* hydrolate caused all formed particles to have a neutral isoelectric point at pH 7. Optimizing particle diameter contributes to the choice of the best technique and to the quantity of each material used in this study. This optimization process has the potential to significantly contribute to the advancement of research into the innovation of encapsulation of lipophilic compounds.

Acknowledgments

The authors acknowledge the Laboratory of Chromatographic and Spectroscopic Analysis (LACE/IFPR, Brazil), the company Anton Paar, the Federal Institute of Paraná, the Federal Institute of Goiás - Rio Verde Campus, and the Federal Technological University of Paraná - Campo Mourão Campus, for providing resources for the research reported in this article.

References

Aćimović, M., Tešević, V., Smiljanić, K., Cvetković, M., Stanković, J., Kiprovski, B., & Sikora, V. (2020). Hydrolates: By-products of essential oil distillation: Chemical composition, biological activity and potential uses. *Advanced Technologies*, *9*(2), 54-70. DOI: https://doi.org/10.5937/savteh2002054a

Becker Peres, L., Becker Peres, L., de Araújo, P. H. H., & Sayer, C. (2016). Solid lipid nanoparticles for encapsulation of hydrophilic drugs by an organic solvent free double emulsion technique. *Colloids and Surfaces B: Biointerfaces*, *140*, 317-323. DOI: https://doi.org/10.1016/j.colsurfb.2015.12.033

Behbahani, E. S., Ghaedi, M., Abbaspour, M., & Rostamizadeh, K. (2017). Optimization and characterization of ultrasound assisted preparation of curcumin-loaded solid lipid nanoparticles: Application of central composite design, thermal analysis and X-ray diffraction techniques. *Ultrasonics Sonochemistry*, *38*, 271-280. DOI: https://doi.org/10.1016/j.ultsonch.2017.03.013

Bot, F., Cossuta, D., & O'Mahony, J. A. (2021). Inter-relationships between composition, physicochemical properties and functionality of lecithin ingredients. *Trends in Food Science and Technology*, *111*, 261-270. DOI: https://doi.org/10.1016/j.tifs.2021.02.028

Comin, V. M., Lopes, L. Q. S., Quatrin, P. M., de Souza, M. E., Bonez, P. C., Pintos, F. G., ... Santos, R. C. V. (2016). Influence of Melaleuca alternifolia oil nanoparticles on aspects of Pseudomonas aeruginosa biofilm. *Microbial Pathogenesis*, *93*, 120-125. DOI: https://doi.org/10.1016/j.micpath.2016.01.019

Coşanay, H., Selimefendigil, F., Öztop, H. F., & Sarı, A. (2022). Experimental Analysis of Melting Behavior of Capric Acid (CA)–Stearic Acid (SA) Eutectic Mixture and its 3D Numerical Solution of Natural Convection in a Cup. *Arabian Journal for Science and Engineering*, *47*(12), 15575-15589. DOI: https://doi.org/10.1007/s13369-022-06719-3

de Sousa, M., & Pessine, F. B. T. (2014). Production of Mannosylated Solid Lipid Nanoparticles to Deliver the Anti-Retroviral Drugs: Efavirenz and Nevirapine. *Advanced Science, Engineering and Medicine*, *6*(10), 1135-1142. DOI: https://doi.org/10.1166/asem.2014.1613

de Souza, I. D. L., Saez, V., de Campos, V. E. B., & Mansur, C. R. E. (2019). Size and Vitamin E Release of Nanostructured Lipid Carriers with Different Liquid Lipids, Surfactants and Preparation Methods. *Macromolecular Symposia*, *383*. DOI: https://doi.org/10.1002/masy.201800011

Gadhave, A. (2014). Determination of Hydrophilic-Lipophilic Balance Value. *International Journal of Science and Research*, *3*(4), 573-575.

Hatefi, L., & Farhadian, N. (2020). A safe and efficient method for encapsulation of ferrous sulfate in solid lipid nanoparticle for non-oxidation and sustained iron delivery. *Colloids and Interface Science Communications*, *34*. DOI: https://doi.org/10.1016/j.colcom.2019.100227

Houghton, P. (2004). Fundamentals of Pharmacognosy and Phytotherapy. *Journal of Ethnopharmacology*, *91*, 177. DOI: https://doi.org/10.1016/j.jep.2003.12.014

Ife, A. F., Harding, I. H., Shah, R. M., Palombo, E. A., & Eldridge, D. S. (2018). Effect of pH and electrolytes on the colloidal stability of stearic acid–based lipid nanoparticles. *Journal of Nanoparticle Research*, *20*(318). DOI: https://doi.org/10.1007/s11051-018-4425-x

Iwundu, M. P., & Oko, E. T. (2021). Design Efficiency and Optimal Values of Replicated Central Composite Designs with Full Factorial Portions. *African Journal of Mathematics and Statistics Studies*, *4*(3), 89-117. DOI: https://doi.org/10.52589/ajmss-ajwdyp0v

Komaiko, J., Sastrosubroto, A., & McClements, D. J. (2015). Formation of Oil-in-Water Emulsions from Natural Emulsifiers Using Spontaneous Emulsification: Sunflower Phospholipids. *Journal of Agricultural and Food Chemistry*, *63*(45), 10078-10088. DOI: https://doi.org/10.1021/acs.jafc.5b03824

Kumar, S., & Randhawa, J. K. (2015). Solid lipid nanoparticles of stearic acid for the drug delivery of paliperidone. *RSC Advances*, *5*(84), 68743-68750. DOI: https://doi.org/10.1039/c5ra10642g

Lian, H., Peng, Y., Shi, J., & Wang, Q. (2019). Effect of emulsifier hydrophilic-lipophilic balance (HLB) on the release of thyme essential oil from chitosan films. *Food Hydrocolloids*, *97*. DOI: https://doi.org/10.1016/j.foodhyd.2019.105213

Ma, H. L., Varanda, L. C., Perussi, J. R., & Carrilho, E. (2021). Hypericin-loaded oil-in-water nanoemulsion synthesized by ultrasonication process enhances photodynamic therapy efficiency. *Journal of Photochemistry and Photobiology B: Biology*, *223*. DOI: https://doi.org/10.1016/j.jphotobiol.2021.112303

McClements, D. J. (2020). Advances in nanoparticle and microparticle delivery systems for increasing the dispersibility, stability, and bioactivity of phytochemicals. *Biotechnology Advances*, *38,* 107287. DOI: https://doi.org/10.1016/j.biotechadv.2018.08.004

Mohite, P., Singh, S., Pawar, A., Sangale, A., & Prajapati, B. G. (2023). Lipid-based oral formulation in capsules to improve the delivery of poorly water-soluble drugs. *Frontiers in Drug Delivery*, *3*. DOI: https://doi.org/10.3389/fddev.2023.1232012

Montgomery, D. C. (2012). Design and Analysis of Experiments Eighth Edition. In *Design*, 2. DOI: https://doi.org/10.1198/tech.2006.s372

Musakhanian, J., Rodier, J. D., & Dave, M. (2022). Oxidative Stability in Lipid Formulations: a Review of the Mechanisms, Drivers, and Inhibitors of Oxidation. *AAPS PharmSciTech*, *23*(151). DOI: https://doi.org/10.1208/s12249-022-02282-0

Naccari, C., Cicero, N., Orlandella, B. M., Naccari, V., & Palma, E. (2023). Antimicrobial activity of essential oils (Citrus bergamia Risso & Poiteau, Melaleuca alternifolia and Chenopodium botrys) on pathogen strains isolated in milk samples from mastitic sheep. *Natural Product Research*, DOI: https://doi.org/10.1080/14786419.2023.2300041

Patil, S. M., Chandra, S. J., Jayanthi, M. K., Shirahatti, P. S., & Ramu, R. (2021). Role of medicinal plants in the treatment of eumycetoma: A review. *Journal of Applied Biology and Biotechnology*, *9*(5), 176-185. DOI: https://doi.org/10.7324/JABB.2021.9524

Pinto, F., de Barros, D. P. C., Reis, C., & Fonseca, L. P. (2019). Optimization of nanostructured lipid carriers loaded with retinoids by central composite design. *Journal of Molecular Liquids*, *293*. DOI: https://doi.org/10.1016/j.molliq.2019.111468

Reis, L. V. de C., Leão, K. M. M., Ribeiro, A. P. B., de Jesus, M. B., Macedo, G. A., & Macedo, J. A. (2020). Evaluation of cytotoxicity of nanolipid carriers with structured Buriti oil in the Caco-2 and $HepG_2$ cell lines. *Bioprocess and Biosystems Engineering*, *43*(6), 1105-1118. DOI: https://doi.org/10.1007/s00449-020-02308-6

Sánchez-Navarro, M. M., Cuesta-Garrote, N., Arán-Áis, F., & Orgilés-Barceló, C. (2011). Microencapsulation of melaleuca alternifolia (tea tree) oil as biocide for footwear applications. *Journal of Dispersion Science and Technology*, *32*(12), 1722-1727. DOI: https://doi.org/10.1080/01932691.2011.616126

Shah, R. M., Eldridge, D. S., Palombo, E. A., & Harding, I. H. (2017). Microwave-assisted microemulsion technique for production of miconazole nitrate- and econazole nitrate-loaded solid lipid nanoparticles. *European Journal of Pharmaceutics and Biopharmaceutics*, *117*, 141-150. DOI: https://doi.org/10.1016/j.ejpb.2017.04.007

Suhaimi, S. H., Hisam, R. H., & Rosli, N. A. (2015). Effects of Formulation Parameters on Particle Size and Polydispersity Index of Orthosiphon Stamineus Loaded Nanostructured Lipid Carrier. *Journal of Advanced in Applied Sciences and Engineering Technology*, *1*, 36-39.

Upadhyay, P., Malik, P., & Upadhyay, S. (2023). Tea tree (Melaleuca alternifolia) Essential Oil Concentration in Microemulsion with Antibacterial and Antifungal Activity: An Overview. *Current Drug Therapy*, *18*(4), 298-311. DOI: https://doi.org/10.2174/1574885518666230228103854

Valarini Junior, O., Cardoso, F. A. R., de Souza, G. B. M., Machado Giufrida, W., & Cardozo-Filho, L. (2021). Single step encapsulation process of ivermectin in biocompatible polymer using a supercritical antisolvent system process. *Asia-Pacific Journal of Chemical Engineering*, *16*(5), 1-14. DOI: https://doi.org/10.1002/apj.2672

Valarini Junior, O., Cardoso, F. A. R., Machado Giufrida, W., de Souza, M. F., & Cardozo-Filho, L. (2019). Production and computational fluid dynamics-based modeling of PMMA nanoparticles impregnated with ivermectin by a supercritical antisolvent process. *Journal of CO_2 Utilization*, *35*, 47-58. DOI: https://doi.org/10.1016/j.jcou.2019.08.025

Voelker, J., Mauleon, R., & Shepherd, M. (2023). The terpene synthase genes of Melaleuca alternifolia (tea tree) and comparative gene family analysis among Myrtaceae essential oil crops. *Plant Systematics and Evolution*, *309*(13). DOI: https://doi.org/10.1007/s00606-023-01847-1

Xu, L., Wang, X., Liu, Y., Yang, G., Falconer, R. J., & Zhao, C. X. (2022). Lipid Nanoparticles for Drug Delivery. *Advanced NanoBiomed Research*, *2*(2). DOI: https://doi.org/10.1002/anbr.202100109

Yamamoto, K., Saito, I., Amaike, Y., Nakaya, T., Ohshita, J., & Gunji, T. (2023). Gel structure and water desalination properties of divinylpyrazine-bridged polysilsesquioxanes. *Journal of Sol-Gel Science and Technology*. DOI: https://doi.org/10.1007/s10971-022-06017-2

Zhang, X., Guo, Y., Guo, L., Jiang, H., & Ji, Q. (2018). In vitro evaluation of antioxidant and antimicrobial activities of melaleuca alternifolia essential oil. *BioMed Research International*, *2018*. DOI: https://doi.org/10.1155/2018/2396109